Effect of doxorubicin on viability and Bax, Bcl-2, p53, Nanog, Sox-2, Oct-4 gene expressions in MCF-7 stem-like cells

Cenk A Andac (cenk_andac@yahoo.com)
Yeditepe University
Nadir Kocak
Selçuk University
Altay Burak Dalan
Yeditepe University
Sena Caglar
Istanbul University
Seyfullah O Arslan
Ankara Yıldırım Beyazıt University

Research Article

Keywords: MCF-7 cancer stem cells, doxorubicin, pluripotency, self-renewal, necrosis, apoptosis

Posted Date: March 31st, 2023

DOI: https://doi.org/10.21203/rs.3.rs-2677263/v1

Abstract

Background: The aim of this study is to clarify whether cell viability, cell death, and gene expressions pertaining to self-renewal and pluripotency differ in doxorubicin (DOX) [IC_{50}] treated and untreated human MCF-7 mammalian cancer cells as well as between their $CD44^{+}/CD24^{-/low}$ cancer stem cells (CSC).

Methods: Non-tumorigenic human MCF-10A mammalian cells and their $CD44^{+}/CD24^{-/low}$ stem cells were used as the control. Cell viability, apoptosis, necrosis and cell death were studied by flow cytometry. Cell death pathways, multidrug resistance, pluripotency and self-renewal were studied at Nanog, Oct-4, Sox-2, p53, Bcl-2 and Bax mRNA gene expression level by qRT-PCR.

Results: IC_{50} value for DOX treated MCF-7 cells was found to be 3.73 μM. Bax, Bcl-2, p53 genes were down-regulated while Nanog, Oct-4, Sox-2 genes were up-regulated in DOX [IC_{50}] treated MCF-7 CSCs. Bax, p53, Nanog, Oct-4 genes were down-regulated while Sox-2, Bcl-2 genes were up-regulated in DOX [IC_{50}] untreated MCF-7 CSCs.

Discussion: In addition to literature reports on DOX [IC_{50}] treated non-stem MCF-7 cells undergoing autophagy and DOX [IC_{50}] treated dedifferentiated MCF-7 ($CD44^{+}/CD24^{-/low}$) cancer stem-like cells undergoing apoptosis, our laboratory data strongly suggest that DOX [IC_{50}] treated MCF-7 CSCs also undergo necrosis as determined by flow cytometry and necroptosis due to downregulation of Bax, Bcl-2 and p53 genes.

Conclusion: Our finding suggests that multiple types of cell death pathways, including apoptosis, necrosis and necroptosis, is involved in DOX [IC_{50}] treated MCF-7 CSCs. DOX [IC_{50}] treated MCF-7 CSCs become pluripotent with self-renewal capability by up-regulation of Nanog, Oct-4, Sox-2 gene expressions to possibly survive necroptosis. Nanog, Oct-4, Sox-2 gene expressions are all down-regulated in DOX [IC_{50}] treated MCF-10A ($CD44^{+}/CD24^{-/low}$) stem cells, disabling the self-renewal and pluripotency features.

Background

Standard treatment options for breast cancer cases involve surgery, radiation therapy, chemotherapy (e.g., anthracyclines such as doxorubicin and epirubicin, cyclophosphamide, platinum agents such as cisplatin and carboplatin, 5-fluorouracil, taxanes such as docetaxel and paclitaxel, vinorelbine, gemcitabine, etc.) [1] and hormone therapy (e.g., tamoxifen for ER^{+} patients, trastuzumab or pertuzumab for $Her2^{+}$ patients) [1]. However, in most of breast cancer cases current conventional chemotherapy regime fails to completely destroy tumour growth as cancer may recur or even metastasize sometime after chemotherapy [2]. Only 60–80% of primary breast cancers and about 50% of metastatic patients respond to chemotherapy treatment [3, 4]. In breast cancer alone, nearly 50% of patients demonstrate primary and/or secondary resistance to doxorubicin [5]. Statistically, about ~ 7–70% of patients were reported in the past to relapse within 5 years after chemotherapy [2].

It has been established that a cancer tumour is comprised of heterogeneous phenotypes [6], enabling some of the cancer cells in the tumour to gain resistance towards chemotherapy by shifting amongst nine interconnected growth pathways, [7] which are apoptosis, proliferation, immune evasion, treatment resistance, metastasis, angiogenesis, differentiation, cell-to-cell communication, and immortality [8]. Even though targeted drug therapy against eight hallmarks of cancer (namely sustained proliferative signalling, evading growth suppressors, activating invasion and metastasis, enabling replicative immortality, inducing angiogenesis, resisting cell death, genomic instability, and tumour-promoting inflammation [8, 9] has been recently in development, experimental data show that a cancer cell has the ability to decrease the phenotype of a hallmark while increasing phenotypes of other hallmarks [10]. Moreover, the presence of crosstalk amongst interconnected signalling pathways further complicates chemotherapy treatment of cancer. After recognition of the crosstalk amongst different signalling pathways, Hanahan [11] suggested that ideally all the cancer hallmark capabilities be targeted for proper treatment of cancer patients.

It was reported by Block et al. [8] that resistance to apoptosis is highly associated with overexpression of Bcl-2 (B-cell lymphoma) family proteins while resistance to necrosis and autophagy do also exist. Therefore, strategies not only against Bcl-2 homology domain 3 but also against activation of autophagy, necrosis and senescence are currently in development [8]. Because highest tolerated doses of chemotherapy fail to completely eradicate tumour cells, it is suggested that a combined use of chemotherapeutic agents be used simultaneously to handle obstacles regarding apoptosis, necrosis, autophagy and senescence [8] and increase therapeutic efficiency.

The fact that a monotherapy regimen does not completely eradicate tumour and that cancer relapses sometime after chemotherapy has led to broad-spectrum multi-therapies as well as more intensive researches to further look into heterogeneous phenotypes of cancer cells in tumour. Accumulating experimental evidences confirming the notion that cancer cells originate from cancer stem cells have shifted the cancer research field towards cancer stem cells. It has been well established that anticancer agents have a sizeable amount of impact on cancer cells but not on cancer stem cells, while they are also cytotoxic to non-tumorigenic cells [12]. Increasing in vitro findings strongly suggest that post-chemotherapy recurrence emanates from cancer stem cells (CSC) which develop resistance to chemotherapeutic agents used [13].

CSCs in breast tumours were initially reported in 2003 by Al-Hajj et al. [14], who observed that breast cancer stem cells enriched in ($CD44^+/CD24^{-/low}$) and $CD44^+/CD24^{-/low}/ESA^+$ phenotypes, as low as 5000 cells, were highly tumorigenic in SCID mice. Later studies showed that $CD44^+/CD24^{-/low}/ESA^+$ tumour initiating breast cancer cells are cancer stem-like (CSL) cells that are able to self-renew, differentiate and become resistant to chemotherapy [15]. For instance; Tsou et al. [16] reported that development of resistance by doxorubicin (DOX, Adriamycin), an anthracyclin drug that interferes with DNA replication by both intercalation of DNA and inhibition of topoisomerase II, in MCF-7 invasive breast ductal carcinoma cells is concentration dependent and associated with mutations in DNA repair system, stem-like cancer

cell properties, EMT properties as well as increased expressions of ATP binding cassette (ABC) transporters (P-glycoprotein) [17, 18] and detoxifying genes such as glutathione-S-transferase-π [16].

In a variety of cancer cell lines, DOX has been shown to induce different types of cell death/growth arrest including apoptosis [19], mitotic catastrophe through inhibition of apoptosis by overexpression of Bcl-2 [20], necrosis [21], drug-induced senescence [22], autophagy [23], differentiation [24] and oxidative stress [25]. Akar et al. [26] reported that lower concentrations of DOX trigger autophagic cell death in MCF-7 cells while much higher concentrations of DOX give rise to apoptotic cell death in MCF-7 cells.

At present, it is unclear whether cell death signalling pathways, pathways conferring resistance to chemotherapy in MCF-7 ($CD44^{+}/CD24^{-/low}$) cancer stem cells as well as their mechanisms for becoming self-renewal and undifferentiated significantly differ from mature MCF-7 cancer cells. Here, we studied DOX-treated and untreated MCF-7 CSCs in terms of Nanog, Oct-4, Sox-2, p53, Bcl-2 and Bax mRNA gene expressions to shed light onto cell death pathway, resistance, differentiation and self-renewal. Information gained here at the genetics level is hoped to help researchers develop novel chemotherapeutic strategies at the stem cell level against breast cancer.

Methods

Cells and reagents

MCF-7 (ER^{+}/PR^{+}) human breast ductal adenocarcinoma and MCF-10A (ER^{-}/PR^{-}) non-tumorigenic epithelial (as the control) cell lines were acquired from ATCC (American Type Culture Collection, Rockville, MD, USA). PBS was purchased from Gibco by Invitrogen of Thermo Scientific (Rockford, USA.). Cell culture media RPMI 1640 was purchased from Biochrome (Bremen, Germany), which was later supplemented with 10% FCS (fetal calf serum) as well as 1% penicillin (100 U/mL) and streptomycin (100 µg/mL) before use. 0.25% Trypsin-EDTA was purchased from Biochrome (Bremen, Germany). HBSS buffer was purchased from ThermoFisher Scientific (Gloucester, UK), which was supplemented with 2% FBS as needed. Fluorochrome FITC-conjugated CD44 and fluorescent PE-conjugated CD24 clones of monoclonal antibodies were purchased from ThermoFisher Scientific, (Gloucester, UK). FITC Annexin V Apoptosis Detection Kit II was purchased from BD Biosciences (Heidelberg, Germany). 0.04% trypan blue dye (2X) was purchased from ThermoFisher Scientific (Gloucester, UK). DMEM/F-12 medium was purchased from ThermoFisher Scientific (Gloucester, UK). Culture plates were purchased from ThermoFisher Scientific (Gloucester, UK). MTT kit was purchased from Promega (Madison, WI, USA). TRIZOL was purchased from ThermoFisher Scientific (Gloucester, UK). Cell culture dishes were purchased from ThermoFisher Scientific (Gloucester, UK). RevertAid First Strand cDNA Synthesis kit was purchased from ThermoFischer Scientific (Gloucester, UK). Binding buffer was purchased from BD Biosciences (San Jose, CA, USA).

Cell Culture And Cell Stock

Two cell lines, MCF-7 (ER+/PR+) human breast ductal adenocarcinoma and MCF-10A non-tumorigenic epithelial (as the control) cell lines, were used to study cell inhibition, cell death and gene expression. Cells were cultured in 75 cm^2 cell/tissue culture flaks, containing 9 mL RPMI 1640 culture medium (Biochrome, Bremen, Germany), at 37^oC in a humidified 5% CO_2 + 95% air incubator. Cells grown up to 80% of the culture flasks were washed once with 1x PBS solution (pH 7.4). Cells were then harvested by addition of 2 mL of 0.25% trypsin-EDTA enzyme solution. The trypsin enzyme activity in the harvested cell culture was inhibited by addition of equal volume of RPMI 1640 culture medium. The harvested cells were then used for IC_{50} and flow cytometry studies. Harvested cells not in use were added freezing medium, containing 10% DMSO and 90% FCS, and archived at -80^oC for later use.

Cultured Cell Count

100 µL of a suspension of cultured cells was transferred to a 1.5 mL Eppendorf tube to which 100 µL 0.4% trypan blue dye (2x) was added and gently pipetted in and out. After keeping the dyed cell suspension at room temperature for 5 minutes, 20 µL of the suspension was pipetted onto a hematocytometric lamina. Cells were then counted in 5 allocated areas under an inverted-microscope at 100x magnification. Cell counts in 5 allocated areas were then averaged out. Total viable and dead cell counts were computed as follows:

Cell count/mL = averaged cell count x 20 (dilution factor) x 10^4

Isolation Of Stem Cells

DOX [IC_{50} at optimal incubation time] treated and untreated MCF-10A and MCF-7 cells were harvested, washed with PBS buffer (pH 7.4), re-suspended in HBSS buffer (containing 2% FBS) followed by addition of fluorochrome FITC-conjugated CD44 (10 µL per 10^6 cells) and fluorochrome PE-conjugated CD24 clones of monoclonal antibody (10 µL per 10^6 cells) solutions (in PBS buffer with sucrose) and incubation in dark for 40 minutes. Unbound antibodies were then washed out with PBS buffer (pH 7.4). The remaining antibody-bound cells were centrifuged and re-suspended in HBSS buffer (containing 2% FBS) for use in flow cytometry studies.

Fluorochrome (FITC-conjugated CD44 and/or fluorescent PE-conjugated CD24 clone of monoclonal) antibody tagged MCF-7 ($CD44^+/CD24^{-/low}$) and MCF-10A ($CD44^+/CD24^{-/low}$) stem cells were counted and separated from other cells by a Fluorescence Activated Cell Sorting (FACS/flow cytometry) instrument (BD FACSAriaTM III cell sorter, San Jose, CA, USA).

Colony Formation Of Stem Cells

Colony formation of $CD44^{+}/CD24^{-/low}$ stem cells was determined by Soft Agar Assay. To prepare base agar plates, 1% agar pre-heated in a microwave was cooled down in a 40°C water-bath. DMEM/F12 (2x) medium pre-heated in a 40°C water-bath was mixed with the 1% agar in the water-bath at 40°C (1:1 v/v), from which 1.5 mL aliquots were transferred to 35 mL petri-dishes. To culture cells, a top agar was prepared by heating 0.7% agar in a microwave and then cooling it down in a 40°C water-bath. DMEM/F12 (2x) medium was pre-warmed in the same 40°C water-bath. Five-thousand ($CD44^{+}/CD24^{-/low}$) stem cells/1 mL DMEM/F12 (2x) pre-warmed in a culture medium, five-thousand harvested cells/1 mL DMEM/F12 (2x) pre-warmed in a culture medium (as the positive control), and 1 mL pre-warmed DMEM/F12(2x) culture medium (as the negative control) were separately mixed gently with 0.7% agar, from which 1.5 mL aliquots were poured onto the base agar in dishes. Inoculated plates were incubated in a humidified incubator at 37°C for 10–14 days. Incubated plates were then stained by 0.005% Crystal Violet 0.5 mL per well) for more than 1 hour to count colonies under a dissecting microscope.

Determination Of Ic Concentration

Inhibition of MCF-7 human breast adenocarcinoma cells by doxorubicin was determined by the MTT [3-(4,5-dimethylthiazol-2-yl)-2,5-diphenyltetrazolium bromide] Cell Proliferation Assay kit as described by company protocol (Promega, Madison, WI, USA). $5x10^3$ cells were pipetted into the wells of a group of 92-well plates ($5x10^3$ cells/well), followed by incubation at 37°C for 24 h, 48 h, 72 h and 96 h. After incubation, 10 µL of MTT solution was added to each well on the 92-well plates, followed by incubation for 2.5 hours under CO_2 atmosphere at 37°C. Then, 200 µL of solutions from each wells were transferred to the wells of fresh 96-well plates, whose absorbances were colorimetrically measured at 490 nm by an Elisa Microplate Reader. Plates with the least apoptosis values under optimal condition were selected to be used for MTT inhibition studies. Increasing concentrations of doxorubicin were added sequentially into the wells of selected plates, followed by incubation for 72 h at 37°C. Wells on the plates were then added 10 µL of MTT solution, whose absorbances were colorimetrically measured at 490 nm by an Elisa Microplate Reader. Percent inhibition values (EQ.1), averaged out of three determinations, were then plotted versus corresponding concentrations of doxorubicin followed by generation of the best-fit trend line to determine the IC_{50} concentration at 50% cell inhibition.

Inhibition % = [1-(averaged $OD_{490\ [DOX+MCF\text{-}7]}$ / averaged $OD_{490\ [MCF\text{-}7]}$)]*100 EQ.1

Flow Cytometry Studies

FITC Annexin V Apoptosis Kit II (BD Pharmgen, USA) was used to determine percent apoptosis/necrosis on the MCF-7 and MCF-10A and their $CD44^{+}/CD24^{-/low}$ stem cell lines, all treated with DOX [IC_{50}], by a Fluorescence Activated Cell Sorting (FACS/flow cytometry) instrument (BD FACSAriaTM III cell sorter).

DOX [IC_{50}] treated cells were firstly harvested and washed with PBS buffer (pH 7.4), which were then re-suspended in HBSS (including 2% FBS) culture medium and incubated in dark for 40 minutes in fluorochrome FITC-conjugated CD44 (10 µL per 10^6 cells) and fluorochrome PE-conjugated CD24 monoclonal antibody (10 µL per 10^6 cells) solutions. Unbound antibodies were then washed out with PBS buffer (pH 7.4). The remaining antibody-bound cells were centrifuged, re-suspended in HBSS (including 2% FBS) culture medium and transferred to FACS tubes for flow cytometry studies.

In order to determine percent cell ratios undergoing cell death, apoptosis or necrosis, DOX [IC_{50}] treated cells were harvested and transferred into FACS tubes, which were then washed with phosphate buffered saline (PBS, pH 7.4) solution and centrifuged at 1500g for 5 minutes. Cell pellets were then dissolved in 5 µL Annexin-V and 5 µl propidium iodide (PI) solutions followed by incubation for 20 minutes at room temperature. In order to facilitate antibody binding, incubated cell solutions were diluted with 1 mL binding buffer [BD Biosciences (San Jose, CA)] and 9 mL PBS buffer (pH 7.4), from which 400 µL aliquots were transferred to FACS tubes for flow cytometry analysis. 10,000 events were implemented for each Flow Cytometry experiment. Events for the Annexin-V^-/PI^+ cells were gated in Q1 quadrant for necrotic cells, events for the Annexin-V^+/PI^+ cells were gated in Q2 quadrant for late apoptotic (dead) cells, events for the Annexin-V^-/PI^- cells were gated in Q3 quadrant for viable cells, events for the Annexin-V^+/PI^- cells were gated in Q4 quadrant for early apoptotic cells.

Gene Expression Studies

Total RNA acquisition from cultured cells

Into the wells, containing about 5–10 x 10^6 cells, of cell culture dishes were added 1 mL TRIZOL (Invitrogen) and mixed by pipetting in and out. Cell lysates were then transferred to 1.5 mL Eppendorf tubes and kept at room temperature for 5–10 minutes. This followed addition of 0.2 mL chloroform and vigorous shaking of the Eppendorf tubes for 15 seconds. Eppendorf tubes were then let stand for 2–3 minutes and centrifuged at 12000xg at + 4^oC for 15 minutes. The upper transparent phase (supernatant) in the tubes were transferred to 1.5 mL Eppendorf tubes, to which 0.5 mL isopropanol were then added and flipped over several times. The mixtures were kept at room temperature for 10 minutes and centrifuged at 12000xg at + 4 ^oC for 4–5 minutes. After the supernatant was removed from the Eppendorf tube, the remaining precipitate was added 75% ethanol followed by centrifugation at 7500xg at + 4 ^oC for 5 minutes. After the supernatant was removed, the remaining RNA was dried at room temperature for 15–20 minutes. Dry RNA was then dissolved in 50 µL RNase free ddH_2O by pipetting in and out. Concentration of the total RNA solution, which also includes DNA, were determined using a NanoDrop 2000/2000c spectrophotometer (USA). The total RNA solution (contaminated with DNA) was then stored at -80^oC until use.

cDNA synthesis

cDNAs were synthesized from purified total RNAs by using the RevertAid First Strand cDNA Synthesis kit (Thermoscientific, USA). In order for the DNA decontamination of total RNA solution, to 1 µg of total RNA (contaminated with DNA) was added 1 µL of 10X reaction buffer solution including $MgCl_2$, 1 µL of DNase I solution, and appropriate amount of RNase free ddH_2O to adjust the final volume to 10 µL. After incubation at 37^oC for 30 minutes, DNase in the mixture was inhibited by addition of 1 µL of 50 mM EDTA and incubation at 65^oC for 10 minutes. Decontaminated and non-degraded RNA was confirmed by 1% agarose gel electrophoresis as well as its OD260/280 measurement ratio (found to be between 1.8 and 2.2). To each DNA-free and intact RNA solution (~ 50 ng/µL) were sequentially added 20 µL cDNA synthesis solution with ingredients given in Table 1. The mixture was then consecutively incubated at 65^oC for 5 minutes, at 42^oC for 60 minutes, and at 25^oC for 5 minutes. cDNAs synthesized were stored at – 20^oC until use.

Quantitative determination of gene expression

Gene expressions were determined by quantitative Real-Time Polymerase Chain Reaction (RT-qPCR) using a LightCyclerR 480 II (Roche, Germany) instrument, which conformed to the MIQE (Minimum Information for Publication of Quantitative Real-Time PCR Experiments) guidelines [27]. Optimized RealTime Ready UPL (Universal Probe Library) primer pairs (forward and reverse) for Bax, Bcl-2, p53, Oct-4, Sox-2, Nanog, GAPDH (the reference) gene specific probes were purchased from Roche (Germany), see Table 2 for primer sequences. LightCycler® 480 Probes Master kit, which includes Taq DNA Polymerase as well as dNTPs and probes, was purchased from Roche (Germany). A Universal Probe Library (UPL) RT-qPCR procedure provided by Roche® (Germany), was adapted for normalization of quantification cycle (Cq) as well as amplification of the genes of interest. Efficiencies of the primer pairs as well as the reference gene were confirmed by running RT-qPCR for five different logarithmic dilutions of each primer pairs and the reference gene in presence of equal amount of cDNA, where Cq increments were found to be consistent with dilution ratios. RT-qPCR experiments were implemented, in presence of a primer pair of the target gene and the LightCycler® 480 Probes Master solution, in two steps as follows: 1) a denaturation step at 95^oC for 10 minutes followed by 2) a 40 cycles of amplification step, each cycle running consecutively at 95^oC for 15 seconds (for denaturation), then at 63^oC for 15 seconds (for annealing) and lastly at 72^oC for 15 seconds (for extension).

Table 1.

ΔCq values for the target genes (in DOX [IC_{50}] treated stem cells) and the control genes (in DOX [IC_{50}] untreated stem cells) were determined by EQ.2, where CqTARGET/CONTROL is the Cq value for the target or the control gene, and CqREFERENCE is the Cq value for GAPDH, the reference gene. Cq values for each target and control genes were averaged out of six RT-qPCR determinations. -ΔΔCq values were determined by EQ.3. This followed the computation of fold regulation values as in EQ.4.

$$\Delta Cq_{TARGET/CONTROL} = (Cq_{TARGET/CONTROL} - Cq_{REFERENCE}) \quad EQ.2$$

$-\Delta\Delta Cq = -[(\Delta Cq_{TARGET} - \Delta Cq_{CONTROL})]$ EQ.3

Fold-regulation = $2^{(-\Delta\Delta Ct)}$ EQ.4

Statistical analysis

Data were analysed by GraphPad PrismR v.5 software (http://www.graphpad.com) to determine P values using Fisher's exact test. P values lower than 0.05 were interpreted as statistically significant. Data were averaged out of at least three determinations and presented as the mean ± S.D.

Results

Two cell lines, MCF-10A (ER-/PR-) non-tumorigenic human breast epithelial (as the control) and MCF-7 (ER+/PR+/HER2+) human breast ductal adenocarcinoma (MCF-7), were used to study the effect of doxorubicin (DOX).

Ic Concentration Of Dox

Inhibition concentration of DOX leading to 50% cell-death (DOX[IC_{50}]) in MCF-7 cells was found to be 3.54 μM (at 72 h incubation time) by MTT assay [20]. The IC_{50} concentration and incubation time determined for MCF-7 cells were also used to study the inhibition of MCF-10A cells by DOX.

Effect Of Dox [ic] Treatment On Cell Viability

Using the IC_{50} concentration of DOX and the optimal incubation time given in the previous section, the effect of DOX on MCF-7 and MCF-10A cell death as well as on their $CD44^{+}/CD24^{-/low}$ stem cells was determined by flow cytometry. As seen in Table 2, without DOX treatment, viable MCF-10A ($CD44^{+}/CD24^{-/low}$) non-tumorigenic stem cells and MCF-7 ($CD44^{+}/CD24^{-/low}$) cancer stem cell percent ratios are 0.7% and 2.7%, respectively. Upon treatment with DOX [IC_{50}], viable MCF-10A ($CD44^{+}/CD24^{-/low}$) non-tumorigenic stem cell and MCF-7 ($CD44^{+}/CD24^{-/low}$) tumorigenic stem cell ratios significantly increased up to 3.3% ($P < 0.05$) and 4.2% ($P < 0.05$), respectively. It is highly likely that DOX treatment has given nonstem MCF-7 cancer cells some features of cancer stem-like cell (CSLC) properties [22, 28, 29] to gain resistance. Increased number of viable MCF-10A ($CD44^{+}/CD24^{-/low}$) non-tumorigenic stem cells is likely due to non-tumorigenic epithelial-to-mesenchymal transition (EMT) which confers chemo-resistance upon DOX [IC_{50}] treatment [30]. It should be indicated here that the viable stem cell ratios given in Table 2 do not necessarily inform of cell apoptosis nor necrosis ratios.

Table 2

To what extend DOX [IC_{50}] treatment leads to cell death (late apoptosis), necrosis or apoptosis (early) in MCF-10A and MCF-7 cells was determined by flow cytometry utilizing Annexin-V and propidium iodide

(PI). Phosphatidylserine usually resides on the inner surface of healthy cell membranes. Initiation of cell death translocates phosphatidylserine to the outer surface of the cell membrane. Annexin-V is 35–36 kDa $Ca2^{+}$-dependent protein and exhibits high specificity and binding affinity towards phosphatidylserine on the outer surface of cell membrane in the early stage of apoptosis. Therefore, fluorescent-tagged Annexin-V is used to detect early apoptosis. In the late stage of cell death, the cell membrane becomes more permeable. In that case, the PI dye that binds to DNA in cells is used to identify necrotic or late apoptotic cells. Percent cell death ratios given in Table 3 represent a sum of cells undergoing early and late stages of apoptosis as well as necrosis.

Annexin-V and PI flow cytometry results obtained for the MCF-10A non-tumorigenic cell line in Table 3 indicate that the cell apoptosis/necrosis ratio is 16.5% when DOX is not used (the control) while it is 47.1% ($P < 0.05$, a significant increase) for DOX [IC_{50}]-treated cells. In terms of the MCF-7 cancer cell line, percent cell apoptosis/necrosis ratios were found to be 25.6% for DOX-free cells (the control) and 55.5% ($P < 0.05$) with DOX [IC_{50}] treatment. These data show that DOX is able to kill MCF-7 mammary cancer cells to some extend while it is cytotoxic to healthy MCF-10A human mammary cells, which questions serious side effects of the DOX chemotherapy applied in cancer patients.

Viable MCF-10A and MCF-7 cell and their computed viable stem cell ($CD44^{+}/CD24^{-/low}$) percent ratios w/wo DOX [IC_{50}] treatment is also listed in Table 3. As seen in Table 3, DOX [IC_{50}] treatment significantly decreased the viability of non-tumorigenic MCF-10A cells (52.9%, $P < 0.05$) as compared to DOX-free MCF-10A cells (83.5%). Likewise, DOX [IC_{50}] treatment significantly decreased the viability of MCF-7 cancer cells (45.5%, $P < 0.05$) as compared to DOX-free (the control) cells (74.4%). In terms of stem cell viability, DOX [IC_{50}] treatment increased viable MCF-10A ($CD44^{+}/CD24^{-/low}$) non-tumorigenic stem cells (1.75%, $P < 0.05$) as compared to the control (0.58%), while DOX [IC_{50}] treatment decreased viable MCF-7 ($CD44^{+}/CD24^{-/low}$) cancer stem cells (1.87%, $P < 0.05$) as compared to the control (2.01%).

Stem Cell Separation And Colony Formation

DOX [IC_{50}] untreated (DOX-free) and treated MCF-10A ($CD44^{+}/CD24^{-/low}$) non-tumorigenic stem cells and MCF-7 ($CD44^{+}/CD24^{-/low}$) cancer stem cells were separated from the corresponding cell line by flow cytometry using fluorescently labelled CD44 and CD24 antibodies. Isolated $CD44^{+}/CD24^{-/low}$ stem cells were then confirmed by culturing in soft-agar dishes followed by observation of colonies as exemplified in Fig. 1. As seen in Fig. 1, colonies are observed in soft-agar dishes cultured with DOX [IC_{50}] untreated MCF-10A and MCF-7 cells (the positive control), and DOX [IC_{50}] untreated MCF-10A ($CD44^{+}/CD24^{-/low}$) and MCF-7 ($CD44^{+}/CD24^{-/low}$) stem cells, while no colonies are present in soft-agar dishes cultured with culture medium (the negative control).

Figure 1

Isolation Of Total Rna From Stem Cells

To prevent stem cells from differentiation, it is essential that stem cells not be allowed to stand alone for some time. Therefore, RNA isolation was carried out immediately after $CD44^{+}/CD24^{-/low}$ stem cells were separated by flow cytometry out of DOX [IC_{50}] treated/untreated MCF-10A and MCF-7 cells. A 1% agarose gel electrophoresis picture for total RNAs extracted from DOX-free MCF-10A ($CD44^{+}/CD24^{-/low}$) and DOX-free MCF-7 ($CD44^{+}/CD24^{-/low}$) stem cells is shown in Fig. 2, in which intact 5S, 18S and 28S ribosomal RNAs are clearly seen while no trace of contaminated DNA is observed.

Figure 2

Gene Expressions

In RT-qPCR studies, GAPDH (gylceraldehyde-3-phosphate dehydrogenase) gene, an autophagy gene that triggers glycolysis to increase survival of mammary cancer cells [31, 32], was selected as the housekeeping gene. Bcl-2, Bax, p53, Nanog, Sox-2, Oct-4 gene expressions were quantitatively determined by RT-qPCR. cDNAs of target genes were synthesized from RNAs of $CD44^{+}/CD24^{-/low}$ stem cells, which were isolated by FACS out of DOX [IC_{50}] untreated/treated MCF-10A and MCF-7 cells. Fold regulation charts for gene expressions are shown in Fig. 3 for DOX-free cells and Fig. 4 for DOX [IC_{50}] treated cells. In RT-qPCR experiments, Cq values for the expression of the Bcl-2 gene in DOX [IC_{50}] treated and untreated MCF-10A $CD44^{+}/CD24^{-/low}$ stem cells were omitted due to values lower than the threshold set by the qPCR instrument, which disabled quantification of fold regulation for the down-regulation of the Bcl-2 gene (marked in asterisk in Fig. 3A & 4A).

Gene expressions in DOX-free stem cells

For control studies, Bax, Bcl-2, p53, and Oct-4 gene expressions in DOX-free MCF-10A ($CD44^{+}/CD24^{-/low}$) and DOX-free MCF-7 ($CD44^{+}/CD24^{-/low}$) stem cells were determined by RT-qPCR. As seen in Fig. 3A, Bax gene expression is higher while Bcl-2 gene expression is lower in DOX [IC_{50}] untreated MCF-10A ($CD44^{+}/CD24^{-/low}$) stem cells. On the other hand, Bax gene expression is lower while Bcl-2 gene expression is higher in DOX [IC_{50}] untreated MCF-7 ($CD44^{+}/CD24^{-/low}$) human mammary adenocarcinoma stem cells (Fig. 3B). As illustrated in Fig. 4A&B, p53 gene expression seems to be low in DOX [IC_{50}] untreated MCF-10A ($CD44^{+}/CD24^{-/low}$) and MCF-7 ($CD44^{+}/CD24^{-/low}$) stem cells, respectively. Considering that the p53 gene expression in this study was referenced to GAPDH gene expression, the p53 gene expression is regarded as (2.5 times) higher in DOX [IC_{50}] untreated MCF-7 ($CD44^{+}/CD24^{-/low}$) tumorigenic stem cells (Fig. 3B) as compared to the DOX [IC_{50}] untreated MCF-10A ($CD44^{+}/CD24^{-/low}$) non-tumorigenic stem cells (Fig. 3A). It was also found that the Oct-4 gene expression is lower in intact MCF-7 ($CD44^{+}/CD24^{-/low}$) stem cells while expression of the Oct-4 gene is relatively higher in intact MCF-10A ($CD44^{+}/CD24^{-/low}$) stem cells.

Gene expressions in DOX [IC_{50}] treated stem cells

Bax, Bcl-2, p53, Oct-4, Sox-2, and Nanog gene expressions in DOX [IC_{50}] treated MCF-10A ($CD44^+/CD24^{-/low}$) and MCF-7 ($CD44^+/CD24^{-/low}$) stem cells were determined by RT-qPCR. It was found that DOX [IC_{50}] treated MCF-10A ($CD44^+/CD24^{-/low}$) stem cells gave rise to down-regulation of the Bcl-2 gene and up-regulation of the Bax gene expressions, Fig. 4A. DOX [IC_{50}] treatment in MCF-7 ($CD44^+/CD24^{-/low}$) stem cells down-regulated Bax, Bcl-2, and p53 gene expressions, Fig. 4B.

Nanog, Oct-4, and Sox-2 gene expressions were all down-regulated in DOX [IC_{50}] treated MCF-10A($CD44^+/CD24^{-/low}$) stem cells (Fig. 4A), while DOX [IC_{50}] treatment in MCF-7 ($CD44^+/CD24^{-/low}$) cancer stem cells up-regulated Nanog, Oct-4 and Sox-2 gene expressions (Fig. 4B).

Discussion

Approximately 0.00001-1% of cancer cells are comprised of cancer stem cells [33]. MCF-7 (ER^+/PR^+) cancer stem cells and MCF-10A (ER^-/PR^-) stem cells express mainly CD44 cell surface protein ($CD44^+$) and none/low CD24 cell surface protein ($CD24^{-/low}$), while MCF-7 cancer cells possess mainly CD24 cell surface marker ($CD24^+$) and no CD44 cell surface marker ($CD44^-$).

One of the main futures of a cancer tumour is its heterogeneity, that is, cancer cells as well as CSCs in a tumour have heterogeneous phenotypes (luminal and/or basal) and they have been shown to interconvert [34]. For instance; breast cancer cells such as MCF-7 and MDA-MB-231 without CSC phenotype ($CD44^+/CD24^+$) produces breast CSCs with $CD44^+/CD24^{-/low}$ phenotype in-vitro and in-vivo. [35]. Also, cancer cells undergo epithelial-to-mesenchymal transition (EMT) [34] and exhibit cancer-stem-like phenotype, gaining more invasive, metastatic and chemo-resistant properties [36]. Mesenchymal-to-epithelial transitions (MET), the reversion process of EMT, also exist in CSCs and is known to participate in the stabilization of distant metastasis by allowing cancerous cells to regain epithelial properties and integrate into distant organs [37].

Interestingly, stem-like basal and luminal subpopulations of breast cancer stem cells interconvert [38]. Therefore, it is really hard to say what ratios of the subpopulations of cancer cells will exist after isolation of cancer stem cells (or cancer stem-like cells) using additional specific markers by FACS as the isolated cancer stem cells will interconvert into a phenotypic equilibrium-state. MCF-7 ($CD44^+/CD24^{-/low}$) CSCs indeed represent subpopulations of CSCs that interconvert, as do MCF-7 ($CD44^+/CD24^{-/low}/ESA^+$) or MCF-7 ($CD44^+/CD24^{-/low}/ALDH^+$) CSCs.

As mentioned before, Al-Hajj et al. [14] reported that both $CD44^+/CD24^{-/low}$ and ($CD44^+/CD24^{-/low}/ESA^+$ CSCs are highly tumorigenic and that ($CD44^+/CD24^{-/low}/ESA^+$ CSCs could maintain their tumorigenic potential when serially passaged for long-term. Therefore, the major difference between MCF-7 ($CD44^+/CD24^{-/low}$) and MCF-7 ($CD44^+/CD24^{-/low}$) CSCs is about how long they maintain their durability

and their distributions in tumour. It is clear that MCF-7 ($CD44^+/CD24^{-/low}$) CSC phenotype interconvert and undergo MET much faster than that of the MCF-7 ($CD44^+/CD24^{-/low}/ESA^+$) CSC phenotype. It was, for instance, reported that breast cancer stem cell ($CD44^+/CD24^{-/low}$) phenotype can differentiate into $ALDH^+$ CSC phenotype and vice versa [39], showing bi-directional differentiation process associated with EMT-TME transition. Furthermore, basal-like breast carcinomas are rich in $CD44^+/CD24^{-/low}$ CSCs and are mainly located on the invasive front of tumour, while luminal breast carcinomas mainly contain $ALDH^+$ CSCs and are rather located in the central part of the tumour [39, 40]. It is for this reason that the MCF-7 ($CD44^+/CD24^{-/low}$) CSCs used in this study were lysed immediately (within 3 minutes) after they were sorted out by FACS machine. In our study, the idea behind immediate cell lysis after cell sorting was to prevent interconversions amongst different subpopulations as much as possible.

As mentioned in the section entitled “Effect of DOX [IC_{50}] treatment on cell viability”, increased number of viable MCF-10A ($CD44^+/CD24^{-/low}$) non-tumorigenic stem cells upon DOX [IC_{50}] treatment is likely due to non-tumorigenic epithelial-to-mesenchymal transition (EMT) which confers chemo-resistance [30]. It is interesting that DOX treatment is toxic to non-tumorigenic MCF-10A mammary cells while it increases MCF-10A ($CD44^+/CD24^{-/low}$) stem cells, suggesting that DOX treatment may have a rejuvenating effect after its chemotherapeutic application.

As seen in Fig. 3A and outlined in the section entitled “Gene expressions in DOX-free stem cells”, high Bax and low Bcl-2 gene expressions in DOX-free MCF-10A ($CD44^+/CD24^{-/low}$) stem cells suggest that healthy MCF-10A ($CD44^+/CD24^{-/low}$) non-tumorigenic human mammary stem cells are prone to apoptosis. On the other hand, low Bax and high Bcl-2 gene expressions in DOX [IC_{50}] untreated MCF-7 ($CD44^+/CD24^{-/low}$) human mammary adenocarcinoma stem cells (see Fig. 3B) suggest that these stem cells are likely to turn-on non-apoptotic cell-death pathways such as necroptosis [41] or autophagy [42], a finding that is consistent with statistical information that the Bcl-2 gene is up-regulated to prevent cancer cells from apoptosis in more than 60% of the mammary cancer cases [43]. As shown in Figs. 4A and 4B, p53 gene expressions in DOX-free MCF-10A ($CD44^+/CD24^{-/low}$) and DOX-free MCF-7 ($CD44^+/CD24^{-/low}$) stem cells, respectively, are relatively low. Considering that the p53 gene expression in this study was referenced to GAPDH gene expression, the p53 gene expression is regarded as (2.5 times) higher in DOX [IC_{50}] untreated MCF-7 ($CD44^+/CD24^{-/low}$) tumorigenic stem cells (Fig. 3B) as compared to the DOX [IC_{50}] untreated MCF-10A ($CD44^+/CD24^{-/low}$) non-tumorigenic stem cells (Fig. 3A). The greater expression of the p53 gene in MCF-7 ($CD44^+/CD24^{-/low}$) stem cells further supports the likelihood of caspase-independent necroptosis or autophagy cell death pathways [42]. As compared to the GAPDH gene level, low expression of p53 suppresses autophagy [44], ultimately turning on apoptosis in DOX-free MCF-10A ($CD44^+/CD24^{-/low}$) stem cells (as Bcl-2 gene expression is low) as well as necroptosis in DOX-free MCF-7 $CD44^+/CD24^{-/low}$ stem cells (as Bcl-2 gene expression is high). Indeed, relatively lower expressions of p53, as compared to the GAPDH gene expression level, in the intact stem cells studied here is a result of the pluripotent feature of the stem cells [45–50]. In addition, lower Oct-4 gene expression in DOX-free MCF-7 ($CD44^+/CD24^{-/low}$) stem cells and relatively higher Oct-4 gene expression in DOX-free MCF-10A

($CD44^+/CD24^{-/low}$) stem cells suggest that MCF-10A ($CD44^+/CD24^{-/low}$) non-tumorigenic stem cells have a greater tendency for cell-survival and differentiation in comparison to the MCF-7 ($CD44^+/CD24^{-/low}$) tumorigenic stem cells.

Looking at the gene expression profiles in DOX [IC_{50}] treated stem cells in Fig. 4(A&B), DOX [IC50] treatment in MCF-10A stem cells led to low Bcl-2 and high Bax gene expressions (Fig. 4A), triggering apoptosis, a finding that is similar to its DOX [IC_{50}] untreated counterpart, Fig. 3A. Down-regulation of the Bax and Bcl-2 gene expressions in DOX [IC_{50}] treated MCF-7 ($CD44^+/CD24^{-/low}$) stem cells is thought to trigger caspase-independent autophagy or necroptosis cell death pathways [42].

Furthermore, it was determined that p53 gene expression was severely down-regulated in DOX [IC_{50}] treated MCF-7 ($CD44^+/CD24^{-/low}$) stem cells, proving that necroptosis is preferred over autophagy upon DOX [IC_{50}] treatment, as down-regulation or low levels of p53 suppresses autophagy [44]. The necroptosis cell death pathway preferred by DOX [IC_{50}] treated MCF-7 ($CD44^+/CD24^{-/low}$) stem cells turns out to be a novel finding that has not been reported in literature before. It is known that very low levels of caspase-3 expression increase the threshold for apoptosis in MCF-7 human mammary adenocarcinoma cells as well as in 45–75% of all mammary cancer cases [51, 52]. As cited in the introduction section, lower concentrations of DOX treatment trigger autophagy in MCF-7 cells while much higher concentrations of DOX give rise to apoptosis in MCF-7 cells [26]. It was also reported that DOX as well as tamoxifen treatment leads to autophagy in mammary cancer cells [33, 53], which is thought to be an alternative pathway adopted by cancer cells for protection from apoptosis [54]. Thus, autophagy is more likely to be adopted by mature MCF-7 cells. It is concluded here that DOX treatment in mature MCF-7 cells leads to autophagy based on literature reports [26] while our laboratory data indicate that DOX [IC_{50}] treated MCF-7 ($CD44^+/CD24^{-/low}$) stem cells are likely to undergo necroptosis in addition to the apoptosis and necrosis presented in the section entitled “Effect of DOX [IC_{50}] treatment on cell viability”.

Cancer stem cells (CSC) constitute a small fraction of a tumour mass, which are endowed with self-renewal, pluripotency and multi-drug resistance. Nowadays, the hierarchical CSC model is established on CSC being tumorigenic and differentiated into a tumour which mainly comprises of non-tumorigenic cells [34, 55–57]. Because they possess similar features as normal stem cells, they are more frequently called cancer stem-like (CSL) cells [34, 55–57]. Currently, there are two known possible ways to form CSCs. One is through the formation of CSCs from normal stem cells [34, 55–57] and the other is by dedifferentiation of transformed (differentiated) cancer cells into CSCs [34, 55–57].

It should be pointed out here that data presented in literature regarding autophagy cell death in MCF-7 cells are all based on laboratory studies in mature (non-stem-like) MCF-7 cancer cells. On the other hand, our laboratory findings were all produced from $CD44^+/CD24^{-/low}$ stem cells isolated out of MCF-7 human mammary ductal adenocarcinoma cell line. Perhaps the most relevant research findings ever published belong to Tsou et al. [16, 9], whose gene expression results were based on DOX-induced multidrug resistant MCF-7 cell line exhibiting stem-like features along with epithelial-to-mesenchymal transition

(EMT). In other words, Tsou et al. [16] studied DOX-induced dedifferentiated MCF-7 ($CD44^+/CD24^{-/low}$) cancer stem-like cells. In Tsou et al. Work [16], the DOX-induced dedifferentiated MCF-7 ($CD44^+/CD24^{-/low}$) CSL cells, which over-express p-glycoprotein, were generated by many repeated exposures of wild type MCF-7 cells to sequentially increased concentrations of DOX (11 increments from 1 nM to 1024 nM by doubling concentrations at each increment, which took 3–5 days of incubation time at each increament), ultimately giving rise to a very high resistance index against DOX. On the other hand, the gene expression results presented in this manuscript were collected directly from natural abundance MCF-7 ($CD44^+/CD24^{-/low}$) cancer stem cells treated only once with DOX [IC_{50} (at 72 h incubation time)]. Tsou et al. [16] reported that application of DOX [1024 nM] on DOX-induced dedifferentiated MCF-7 ($CD44^+/CD24^{-/low}$) CSL cells gave rise to down-regulation of Bcl-2 and p53 and slightly up-regulation of Bax expression, leading to a decrease in apoptosis that could not be addressed by the authors. In our laboratory study, DOX [IC_{50}] treated MCF-7 ($CD44^+/CD24^{-/low}$ cancer stem cells undergo apoptosis and necrosis as determined by Flow Cytometry as well as necroptosis due to down-regulation of Bcl-2, Bax and p53 gene expressions. Therefore, based on our laboratory work we hypothesize that although DOX-induced dedifferentiated MCF-7 ($CD44^+/CD24^{-/low}$) CSL cells reported by Tsou et al. [16] and the MCF-7 ($CD44^+/CD24^{-/low}$) cancer stem cells reported here share some similarities in stemness (i.e. over-expression of p-glycoprotein, expression of CD44 marker, etc.), they may differ in their gene expressions depending on what induces dedifferentiation into CSL cells.

As seen in Fig. 4A, down-regulation of Nanog, Oct-4, and Sox-2 gene expressions in DOX [IC_{50}] treated MCF-10A($CD44^+/CD24^{-/low}$) stem cells indicate that non-tumorigenic $CD44^+/CD24^{-/low}$ stem cells lose their self-renewal and pluripotent features although the number of viable MCF-10A ($CD44^+/CD24^{-/low}$) stem cells increase (Table 2) due possibly to non-tumorigenic epithelial-to-mesenchymal transition (EMT) [58]. On the other hand, DOX [IC_{50}] treated MCF-7 ($CD44^+/CD24^{-/low}$) cancer stem cells gave rise to a profile of up-regulation with the Nanog, Oct-4 and Sox-2 gene expressions, Fig. 4B, suggesting that the tumorigenic mammary stem cells become highly pluripotent and gain a self-renewal feature leading to an increase in the number of viable stem cells (Table 2). It is highly likely that DOX [IC_{50}] treated MCF-7 ($CD44^+/CD24^{-/low}$) stem cells increase Oct-4 and Nanog gene expressions to survive necroptosis. Here, down-regulation of p53 in DOX [IC_{50}] treated MCF-7 ($CD44^+/CD24^{-/low}$) stem cells is to increase Nanog gene expression for survival [59].

Conclusion

We implemented flow cytometry and qRT-PCR experiments to determine the effect of DOX [IC_{50} (at 72 h incubation time)] treatment on viability and gene expressions in non-tumorigenic MCF-10A ($CD44^+/CD24^{-/low}$) and tumorigenic MCF-7 ($CD44^+/CD24^{-/low}$) stem cells. It is reported in literature [26] that DOX treated non-stem MCF-7 cells undergo autophagy. Currently, there is no clear information in literature regarding the type of cell deaths MCF-7 ($CD44^+/CD24^{-/low}$) stem cells undergo upon DOX treatment.

Here were report that treatment of MCF-7 ($CD44^{+}/CD24^{-/low}$) stem cells with DOC[IC_{50}] turns-on a cross-talk between apoptosis, necrosis and necroptosis. We also compared our laboratory data on MCF-7 ($CD44^{+}/CD24^{-/low}$) stem cells with those of Tsou et al. [16] laboratory data on dedifferentiated MCF-7 ($CD44^{+}/CD24^{-/low}$) CSL cells and found out a difference at gene expression level in that Bax was reported to be upregulated with a decrease in apoptosis in Tsou et al. [16] work, which was found by our laboratory data to be inconsistent because Bax was down-regulated, highly possibly leading to necroptosis in addition to apoptosis and necrosis determined in our laboratory work.

In terms of pluripotency and self-renewal, DOX [IC_{50}] treated MCF-10A ($CD44^{+}/CD24^{-/low}$) stem cells do not possess self-renewal and pluripotency features while DOX [IC_{50}] treatment leads MCF-7 ($CD44^{+}/CD24^{-/low}$) cancer stem cells to highly gain pluripotency and self-renewal features to survive necroptosis.

Abbreviations

DOX = doxorubicin, adriamycin ; DOX [IC_{50}] = doxorubicin applied at IC_{50} concentration; CSC = cancer stem cells; CSLC = Cancer stem-like cells; EMT = epithelial-to-mesenchymal transition; PI = propidium iodide

Declarations

Ethics approval and consent to participate

Not applicable.

Consent for publication

Not applicable.

Availability of data and materials

The datasets generated and/or analyzed during the current study are not publicly available due feasibility of the study to begin a clinical trial; however, they are available from the corresponding author upon reasonable request.

Conflict of interests

The authors declare that they have no conflict of interests.

Funding

Not applicable

Author's Contribution

C.A. Andac led the research. N. Koçak and C.A. Andac implemented the experiments. All authors analyzed the results. All authors made contributions to the discussion section in the manuscript. C.A. Andac wrote the manuscript. S. Caglar prepared the Figures and Tables. S. Caglar, A.B. Dalan and S.O. Arslan edited the manuscript. S. Caglar formatted the manuscript according to the journal's guidelines. All authors reviewed the manuscript.

Acknowledgement

Not applicable

Author's Information

Not applicable

References

1. Pathak M, Dwivedi SN, Deo SVS, Thakur B, Sreenivas V, Rath GK. Neoadjuvant chemotherapy regimens in treatment of breast cancer: a systematic review and network meta-analysis protocol. Syst Reviews. 2018;7(89):1–8. https://doi.org/10.1111/j.1365-277X.2011.01184.x.
2. Brewster AM, Hortobagyi GN, Broglio KR, Kau SW, Santa-Maria CA, et al. Residual risk of breast cancer recurrence 5 years after adjuvant therapy. J Natl Cancer Inst. 2008;100(16):1179–83. https://doi.org/10.1093/jnci/djn233.
3. Bartsch R, Wenzel C, Steger GG. Trastuzumab in the management of early and advanced stage breast cancer. Biologics: Targets & Therapy. 2007;1(1):19–31.
4. Vici P, Colucci G, Gebbia V, Amodio A, Giotta F, et al. Firstline treatment with epirubicin and vinorelbine in metastatic breast cancer. J Clin Oncol. 2002;20(11):2689–94. https://doi.org/10.1200/JCO.2002.06.039.
5. Mechetner E, Kyshtoobayeva A, Zonis S, Kim H, Stroup R, et al. Levels of multidrug resistance (MD HR1) P-glycoprotein expression by human breast cancer correlate with in vitro resistance to taxol and doxorubicin. Clin Cancer Res. 1998;4(2):389–98.
6. Vogelstein B, Papadoupoulos N, Velculescu VE, Shou S, Diaz LAJr, et al. Cancer genome landscapes Science. 2013;339:1546–58. https://doi.org/10.1126/science.1235122.
7. Zahreddine H, Borden KLB. Mechanisms and insights into drug resistance in cancer. Front Pharmacol. 2013;4:28. https://doi.org/10.3389/fphar.2013.00028.
8. Block KI, Gyllenhaal C, Low L, Amedei A, Amin A, et al. A broad-spectrum integrative design for cancer prevention and therapy. Sem Cancer Biol. 2015;35:276–S304. https://doi.org/10.1016/j.semcancer.2015.08.002.

9. Weinberg RA. Hallmarks of cancer: the next generation. Cell. 2011;144:646–74. https://doi.org/10.1016/j.cell.2011.02.013.
10. Bergers G, Hanahan D. Modes of resistance to anti-angiogenic therapy. Nat Rev Cancer. 2008;8:592–603. https://doi.org/10.1038/nrc2442.
11. Hanahan D. Rethinking the war on cancer. Lancet. 2014;383(9916):558–63. https://doi.org/10.1016/S0140-6736(13)62226-6.
12. Guan Y, Gerhard B, Hogge DE. Detection, isolation and stimulation of quiescent primitive leukemic progenitor cells from patients with acute myeloid leukemia (AML). Blood. 2003;101(8):3142–9. https://doi.org/10.1182/blood-2002-10-3062.
13. Yang F, Xu J, Tang L, Guan X. Breast cancer stem cell: the roles and therapeutic implications. Cell Mol Life Sci. 2017;74(6):951–66. https://doi.org/10.1007/s00018-016-2334-7.
14. Al-Hajj M, Wicha MS, Benito-Hernandez A, Morrison SJ, Clarke MF. Prospective identification of tumorigenic breast cancer cells. Proc Natl Acad Sci USA. 2003;100(7):3983–8. https://doi.org/10.1073/pnas.0530291100.
15. Fillmore CM, Kuperwasser C. Human breast cancer cell lines contain stem-like cells that self-renew, give rise to phenotypically diverse progeny and survive chemotherapy. Breast Cancer Res. 2008;10(2):R25. https://doi.org/10.1186/bcr1982.
16. Tsou SH, Chen TM, Hsiao HT, Chen YH. A critical dose of doxorubicin is required to alter the gene expression profiles in MCF-7 cells acquiring multidrug resistance. PLoS ONE. 2015;10(1):e0116747. https://doi.org/10.1371/journal.pone.0116747.
17. Kovalchuk O, Filkowski J, Meservy J, Ilnytskyy Y, Tryndyak VP, et al. Involvement of microRNA-451 in resistance of the MCF-7 breast cancer cells to chemotherapeutic drug doxorubicin. Mol Cancer Therapy. 2008;7:2152–9. https://doi.org/10.1158/1535-7163.MCT-08-0021.
18. Bao L, Haque A, Jackson K, Hazari S, Moroz K, et al. Increased expression of P-glycoprotein is associated with doxorubicin chemoresistance in the metastatic 4T1 breast cancer model. Am J Pathol. 2011;178(2):838–52. https://doi.org/10.1016/j.ajpath.2012.02.024.
19. Wang S, Konorev EA, Kotamraju S, Joseph J, Kalivendi S, Kalyanaraman B. Doxorubicin induces apoptosis in normal and tumor cells via distinctly different mechanisms. Intermediacy of H2O2- and p53-dependent pathways. J Biol Chem. 2004;279(24):25535–43. https://doi.org/10.1074/jbc.M400944200.
20. Come MG, Skladanowski A, Larsen AK, Laurent G. Dual mechanism of daunorubicin-induced cell death in both sensitive and MDR-resistant HL-60 cells. Br J Cancer. 1999;79:1090–7. https://doi.org/10.1038/sj.bjc.6690174.
21. Hyeon-Jun S, Hyuk-Kwon K, Jae-Hyeok L, Xiangai G, Asma A, et al. Doxorubicin-induced necrosis is mediated by poly-(ADP-ribose) polymerase 1 (PARP1) but is independent of p53. Sci Rep. 2015;5:5798. https://doi.org/10.1038/srep15798.
22. Sliwinska MA, Mosieniak G, Wolanin K, Babik A, Piwocka K, et al. Induction of senescence with doxorubicin leads to increased genomic instability of HCT116 cells. Mech Ageing Dev. 2009;130(1–

2):24–32. https://doi.org/10.1016/j.mad.2008.04.011.

23. Hye PJ, Sung Hyun C, Hyungtae K, Seung TJ, Woong BJ, et al. Doxorubicin regulates autophagy signals via accumulation of cytosolic Ca2 + in human cardiac progenitor cells. Int J Mol Sci. 2016;17:1680. https://doi.org/10.3390/ijms17101680.
24. Branco AF, Sampaio SF, Moreira AC, Holy J, Wallace KB, et al. Differentiation-dependent doxorubicin toxicity on H9c2 cardiomyoblasts. Cardiovasc Toxicol. 2012;12:326–40. https://doi.org/10.1007/s12012-012-9177-8.
25. Gewirtz DA. A critical evaluation of the mechanisms of action proposed for the antitumor effects of the anthracycline antibiotics adriamycin and daunorubicin. Biochem Pharmacol. 1999;57:727–41. https://doi.org/10.1016/S0006-2952(98)00307-4.
26. Akar U, Chaves-Reyez A, Barria M. Silencing of Bcl- 2 expression by small interfering RNA induces autophagic cell death in MCF-7 breast cancer cells. Autophagy. 2008;4(5):669–79. https://doi.org/10.4161/auto.6083.
27. Bustin SA, Benes V, Garson JA, Hellemans J, Huggett J, et al. The MIQE guidelines: Minimum information for publication of quantitative real-time PCR experiments. Clin Chem. 2009;55(4):611–22. https://doi.org/10.1373/clinchem.2008.112797.
28. Olsson E, Honeth G, Bendahl PO, Saal LH, Gruvberger-Saal S, et al. CD44 isoforms are heterogeneously expressed in breast cancer and correlate with tumor subtypes and cancer stem cell markers. BMC Cancer. 2011;11:418. https://doi.org/10.1186/1471-2407-11-418.
29. Bourguignon LY, Xia W, Wong G, Hyaluronan-mediated. CD44 interaction with p300 and SIRT1 regulates beta-catenin signalling and NFkappaB-specific transcription activity leading to MDR1 and BclxL gene expression and chemoresistance in breast tumor cells. J Biol Chem. 2009;284(5):2657–71. https://doi.org/10.1074/jbc.M806708200.
30. Lim S, Becker A, Zimmer A, Lu J, Buettner R, Kirfel J. SNAI1-mediated epithelial-mesenchymal transition and cellular plasticity by regulating genes involved in cell death and stem cell maintenance. PLoS ONE. 2013;8(6):e66558. https://doi.org/10.1371/journal.pone.0066558.
31. Gu Y, Li P, Peng F, Zhang M, Zhang Y, et al. Autophagy-related prognostic signature for breast cancer. Mol Carcinog. 2016;55(3):292–9. https://doi.org/10.1002/mc.22278.
32. Colell A, Ricci JE, Tait S, Milasta S, Maurer U, et al. Green, GAPDH and autophagy preserve survival after apoptotic cytochrome c release in the absence of caspase activation. Cell. 2007;129(5):983–97. https://doi.org/10.1016/j.cell.2007.03.045.
33. Kreso A, Dick JE. Evolution of the cancer stem cell model. Cell Stem Cell. 2014;14:275–91. https://doi.org/10.1016/j.stem.2014.02.006.
34. Palomeras S, Ruiz-Martínez S, Puig T. Targeting breast Cancer stem cells to overcome treatment resistance. Molecules. 2018;23:2193. https://doi.org/10.3390/molecules23092193.
35. Meyer MJ, Fleming JM, Ali MA, Pesesky MW, Ginsburg E, Vonderhaar BK. Dynamic regulation of CD24 and the invasive, CD44posCD24neg phenotype in breast cancer cell lines. Breast Cancer Res. 2009;11(6):R82. https://doi.org/10.1186/bcr2449.

36. Singla M, Kumar A, Bal A, Sarkar S, Bhattacharyya S. Epithelial-to-mesenchymal transition induces stem like phenotype in renal cell carcinoma cells. Cancer Cell Int. 2018;18:57. https://doi.org/10.1186/s12935-018-0555-6.
37. Yang J, Weinberg RA. Epithelial-mesenchimal transition: at the crossroads of development and tumor metastasis. Dev Cell. 2008;14(6):818–26. https://doi.org/10.1016/j.devcel.2008.05.009.
38. Gupta PB, Fillmore CM, Jiang G, Shapira SD, Tao K, Kuperwasser C, Lander ES. Stochastic state transitions give rise to phenotypic equilibrium in populations of cancer cells. Cell. 2011;146:633–44. https://doi.org/10.1016/j.cell.2011.07.026.
39. Liu S, Cong Y, Wang D, Sun Y, Deng L, et al. Breast cancer stem cells transition between epithelial and mesenchymal states reflective of their normal counterparts. Stem Cell Reports. 2013;2:78–91. https://doi.org/10.1016/j.stemcr.2013.11.009.
40. Bissoli I, Muscari C. Doxorubicin and α-mangostin oppositely affect luminal breast cancer cell stemness evaluated by a new retinaldehyde-dependent ALDH assay in MCF-7 tumor spheroids. Biomed Pharmacotherapy. 2020;124:109927. https://doi.org/10.1016/j.biopha.2020.109927.
41. Degterev A, Hitomi J, Germscheid M, Chen IL, Korkina O, et al. Identification of RIP-1 kinase as a specific cellular target of necrostatins. Nat Chem Biol. 2008;4(5):313–21. https://doi.org/10.1038/nchembio.83.
42. Botti J, Djavaheri-Mergny M, Pilatte Y, Codogno P. Autophagy signalling and the cogwheels of cancer. Autophagy. 2006;2(2):67–73. https://doi.org/10.4161/auto.2.2.2458.
43. Dalby KN, Tekedereli I, Lopez-Berestein G, Ozpolat B. Targeting the prodeath and prosurvival functions of autophagy as novel therapeutic strategies in cancer. Autophagy. 2010;6(3):322–9. https://doi.org/10.4161/auto.6.3.11625.
44. Calzone L, Zinovyev A, Zhivotovsky B. Chapter 6: Understanding different types of cell death using systems biology, In: Sytems Biology of Apoptosis; I.N. Lavrik, Ed.; Springer SBM: New York 2013;125:125–143. https://doi.org/10.1007/978-1-4614-4009-3_6
45. Hong H, Takahashi K, Ichisaka T, Aoi T, Kanagawa O, et al. Suppression of induced pluripotent stem cell generation by the p53-p21 pathway. Nature. 2009;460(7259):1132–5. https://doi.org/10.1038/nature08235.
46. Kawamura T, Suzuki J, Wang YV, Menendez S, Morera LB, et al. Linking the p53 tumour suppressor pathway to somatic cell reprogramming. Nature. 2009;460(7259):1140–4. https://doi.org/10.1038/nature08311.
47. Utikal J, Polo JM, Stadtfeld M, Maherali N, Kulalert W, et al. Immortalization eliminates a roadblock during cellular reprogramming into iPS cells. Nature. 2009;460(7259):1145–8. https://doi.org/10.1038/nature08285.
48. Zhao Y, Yin X, Qin H, Zhu F, Liu H, et al. Two supporting factors greatly improve the efficiency of human iPSC generation. Cell Stem Cell. 2008;3(5):475–9. https://doi.org/10.1016/j.stem.2008.10.002.

49. Li H, Collado M, Villasante A, Strati K, Ortega S, et al. The Ink4/Arf locus is a barrier for iPS cell reprogramming. Nature. 2009;460(7259):1136–9. https://doi.org/10.1038/nature08290.
50. Marion RM, Strati K, Li H, Murga M, Blanco R, et al. A p53-mediated DNA damage response limits reprogramming to ensure iPS cell genomic integrity. Nature. 2009;460(7259):1149–53. https://doi.org/10.1038/nature08287.
51. Tobias MN. Cell Death: Apoptosis and Necrosis. Ed., AvE4EvA Publications 2015; 73, ISBN-13: 978-953-51-2236-4.
52. Devarajan E, Chen J, Multani AS, Pathak S, Sahin AA, Mehta K. Human breast cancer MCF-7 cell line contains inherently drug-resistant subclones with distinct genotypic and phenotypic features. Int J Oncol. 2002;20(5):913–20. https://doi.org/10.3892/ijo.20.5.913.
53. Tong XP, Chen Y, Zhang SY, Xie T, Tian M, et al. Key autophagic targets and relevant small-molecule compounds in cancer therapy. Cell Prolif. 2015;48:7–16. https://doi.org/10.1111/cpr.12154.
54. Brech A, Ahlquist T, Lothe RA, Stenmark H. Autophagy in tumor suppression and promotion. Mol Oncol. 2009;3(4):366–75. https://doi.org/10.1016/j.molonc.2009.05.007.
55. Sun Q, Wang Y, Officer A, Pecknold B, Lee G, et al. Stem-like breast cancer cells in the activated state resist genetic stress via TGFBI-ZEB1. NPJ Breast Cancer. 2022;8(1):5. https://doi.org/10.1038/s41523-021-00375-w.
56. Lucero M, Thind J, Sandoval J, Senaati S, Jimenez B, et al. Stem-like cells from invasive breast carcinoma cell line MDA-MB-231 express a distinct set of Eph receptors and Ephrin ligands. Cancer Genomics Proteomics. 2020;17(6):729–38. https://doi.org/10.21873/cgp.20227.
57. Urbaniaka A, Reed MR, Fil D, Moorjani A, Heflin S, et al. Single and double modified salinomycin analogs target stem-like cells in 2D and 3D breast cancer models. Biomed Pharmacother. 2021;141:111815. https://doi.org/10.1016/j.biopha.2021.111815.
58. Zhang T, Zhou H, Wang K, Wang X, Wang M, et al. Role, molecular mechanism and the potential target of breast cancer stem cells in breast cancer development. Biomed Pharmacother. 2022;147:112616. https://doi.org/10.1016/j.biopha.2022.112616.
59. Lin T, Chao C, Saito S, Mazur SJ, Murphy ME, et al. p53 induces differentiation of mouse embryonic stem cells by suppressing Nanog expression. Nat Cell Biol. 2005;7:165–71. https://doi.org/10.1038/ncb1211.

Tables

Tables 1-3 is available in the Supplementary Files section.

Figures

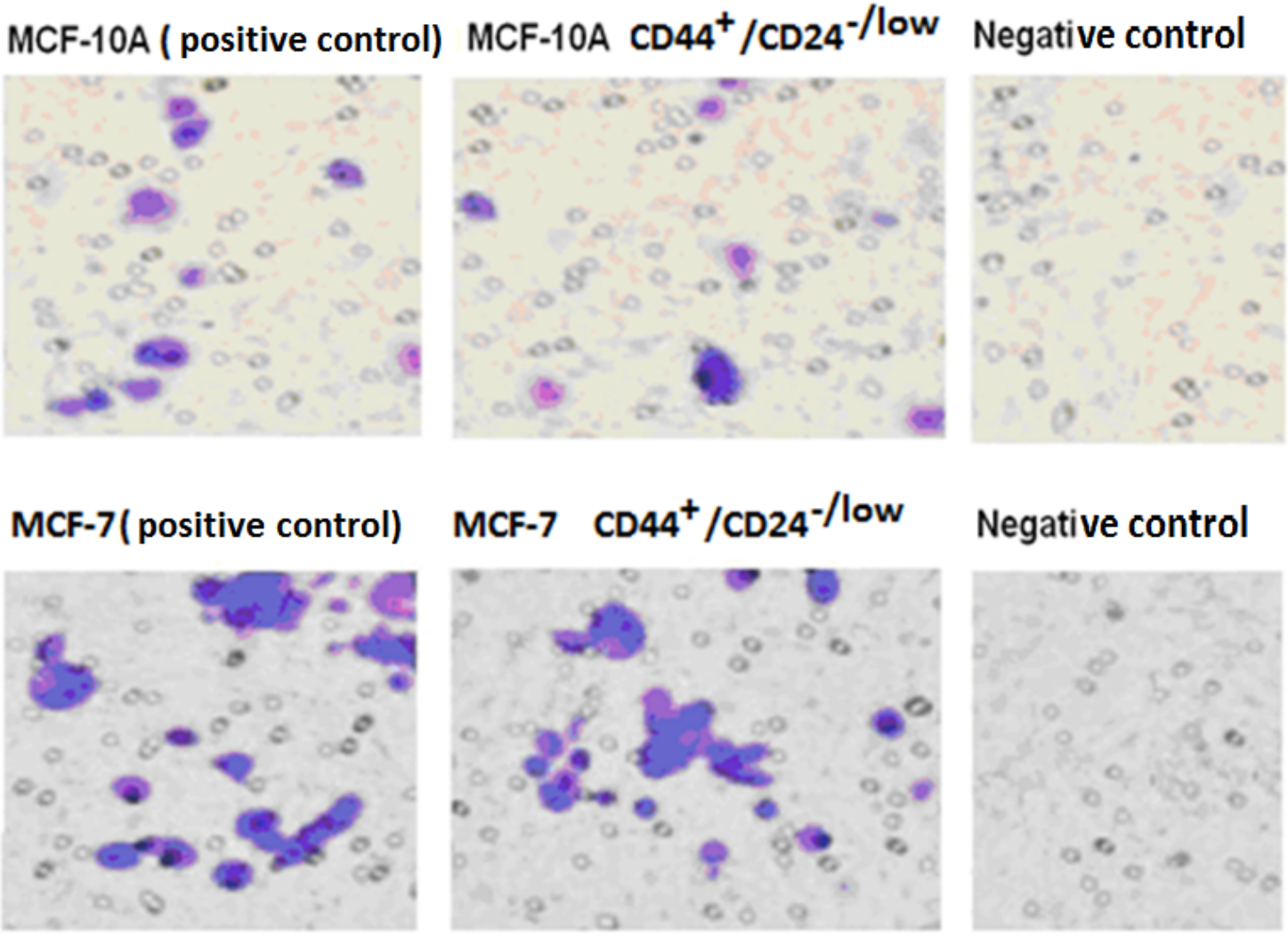

Figure 1

Sample pictures of colony formation (in soft-agar dishes) of DOX-untreated $CD44^{+}/CD24^{-/low}$ stem cells isolated by flow cytometry. Positive control: DOX-untreated MCF-10A and MCF-7 cell lines. Negative control: culture medium.

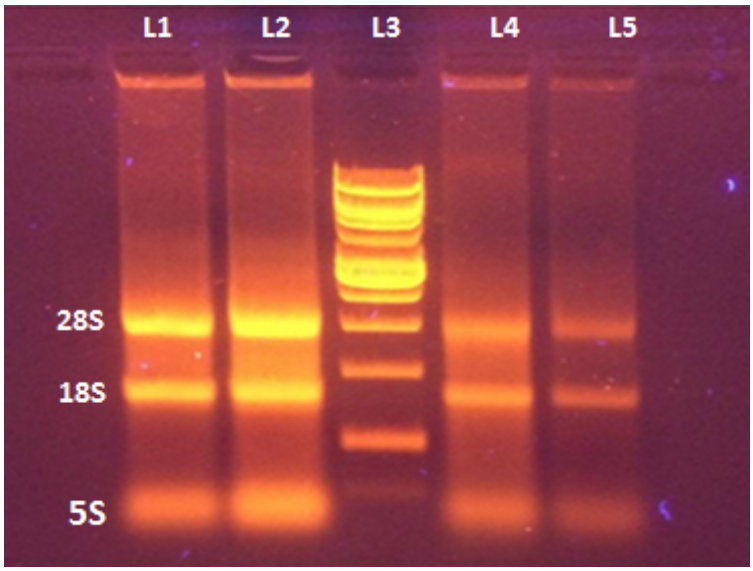

Figure 2

1% agarose gel electrophoresis picture of decontaminated RNA isolate. L1 & L2: Duplicates of a total RNA sample extracted from DOX untreated MCF-10A $CD44^{+}/CD24^{-/low}$ stem cells, L3: Marker [1 kb DNA Ladder (Vivantis, Coast Highway, USA)], and L4 & L5: Duplicates of a total RNA sample extracted from DOX untreated MCF-7 $CD44^{+}/CD24^{-/low}$ stem cells

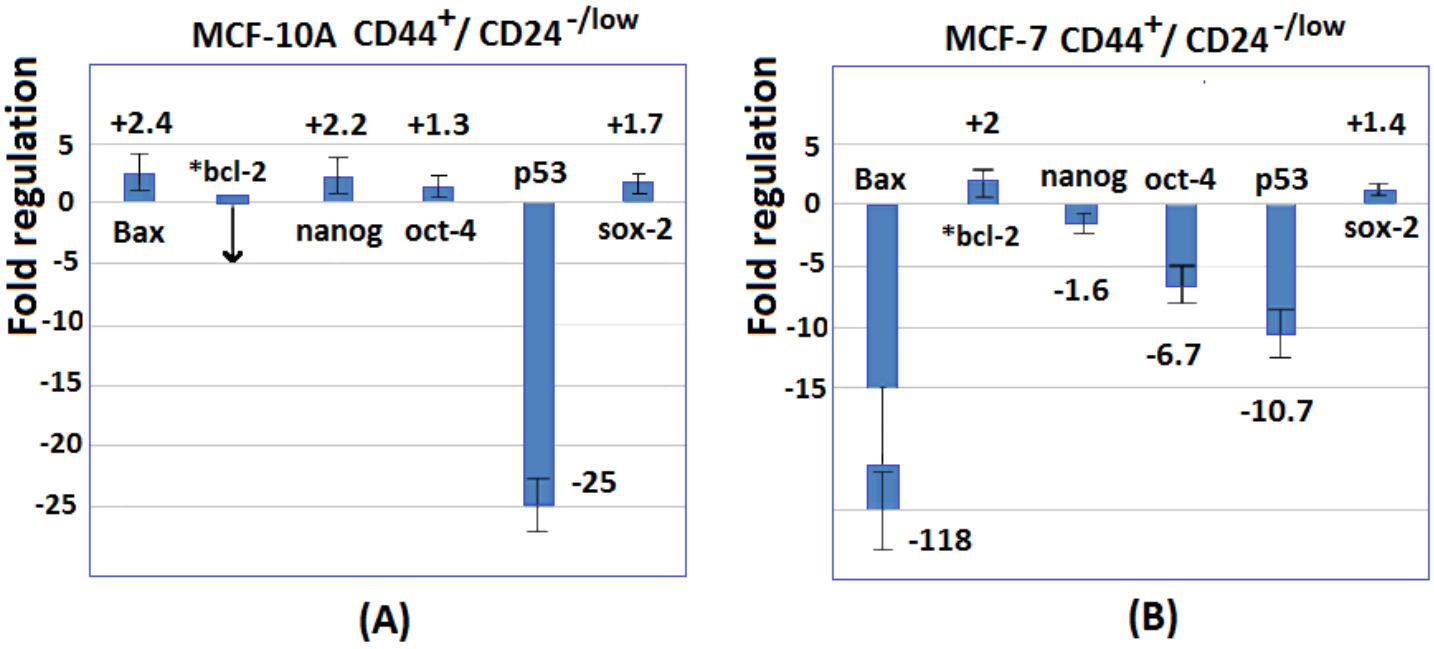

Figure 3

Fold regulation charts for Bax, Bcl-2, Nanog, Oct-4, p53 and Sox-2 gene expressions in DOX[IC_{50}] untreated (A) MCF-10A $CD44^{+}/CD24^{-/low}$ stem cells and (B) MCF-7 $CD44^{+}/CD24^{-/low}$ stem cells. All gene

expressions were referenced to the GAPDH gene expression. * : Fold regulation value for down-regulation can not be computed by EQ.4.

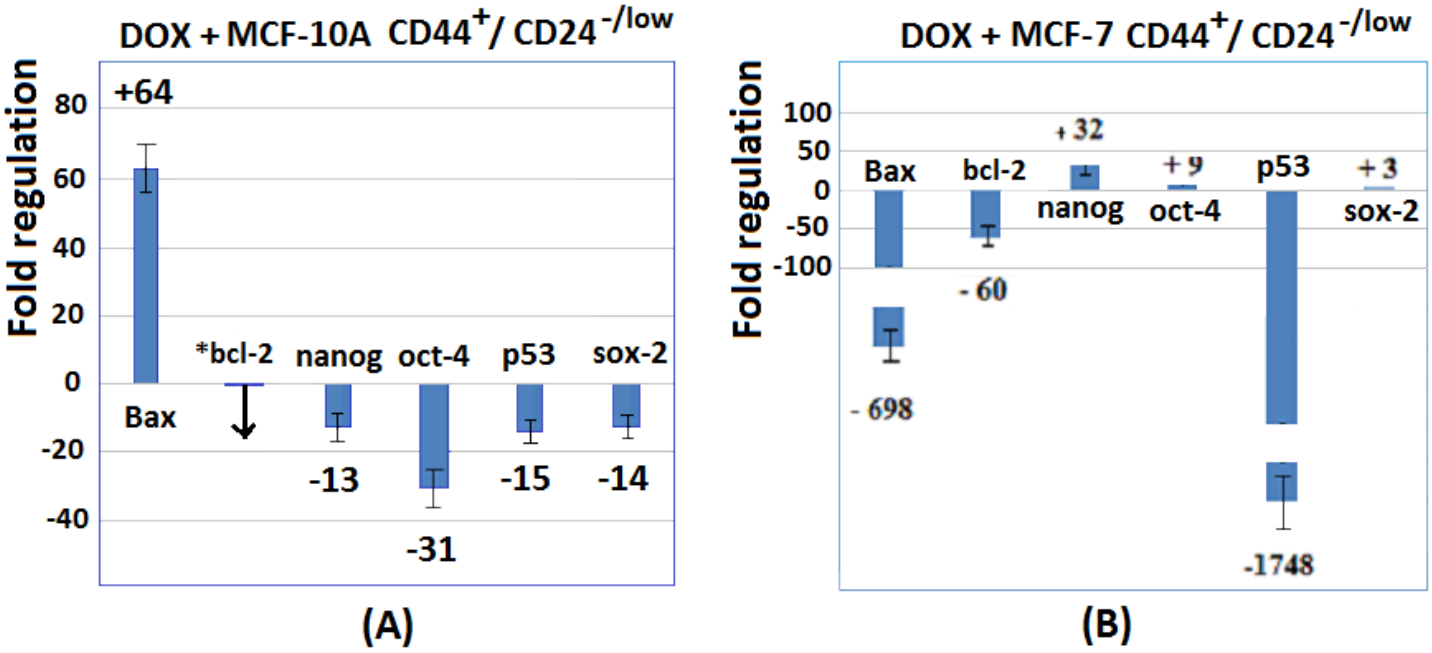

Figure 4

Fold regulation charts for Bax, Bcl-2, Nanog, Oct-4, p53 and Sox-2 gene expressions in DOX[IC_{50}] treated (A) MCF-10A $CD44^{+}/CD24^{-/low}$ stem cells and (B) MCF-7 $CD44^{+}/CD24^{-/low}$ stem cells. All gene expressions were referenced to the GAPDH gene expression. * : Fold regulation value for down-regulation can not be computed by EQ.4.

Supplementary Files

This is a list of supplementary files associated with this preprint. Click to download.

- Tablesandlegends.docx